

**CHAPTER IV**  
**A STUDY OF CA-ATMP PRECIPITATION**  
**IN THE PRESENCE OF MAGNESIUM ION**

**4.1 Abstract**

ATMP (aminotri (methylenephosphonic acid)), a phosphonate scale inhibitor used in the petroleum industry, was used as a model scale inhibitor in this study. One of the goals of this work was to determine the range of conditions under which Mg ions, which are formed in reservoir formations containing dolomite, modulate the formation of Ca-ATMP precipitate as a scale inhibitor. The results revealed that the amount of ATMP precipitated decreased with addition of Mg ions in solution at all values of the solution pH. Furthermore, an increase in both the solution pH and the concentration of the divalent cations in solution resulted in a change of the molar ratio of (Ca+Mg) to ATMP in the precipitates. At a low solution pH (pH 1.5) Mg ions had little effect on composition of Ca-ATMP precipitate. However, at higher values of the solution pH (pH 4 and 7), the Ca to ATMP molar ratio in the precipitates decreased with increasing concentration of the Mg. Here it was found that Mg ions replaced Ca ions on available reactive sites of ATMP molecules. These results determined the limits of Mg ion concentration, which effects the precipitation of Ca-ATMP, Mg-ATMP, and (Ca+Mg)-ATMP. The dissolution of the scale inhibitors was studied using a rotating disk reactor. These experiments showed that the total divalent cation molar ratio (Ca+Mg) to ATMP in the precipitates is the primary factor that controls the rate of dissolution (release) of the phosphonate precipitates. The phosphonate precipitate dissolution rates decreased as the molar ratio of divalent cations to ATMP in the precipitates increased.

## 4.2 Introduction

One of the most effective methods used in oilfield operations to prevent or limit scale formation is the use of squeeze treatments. A squeeze treatment is a procedure where scale inhibitors are injected into the formation and then shut in for a period of time. Precipitation and adsorption squeeze treatments are the two major types of squeeze treatments, each having a different dominant retention/release mechanism. Because it has been previously shown that precipitation squeeze treatments offer longer squeeze lifetimes (Carlberg, 1987; Oddo and Tomson, 1994), thus this chapter focused only on precipitation. In precipitation squeeze treatments, the injected scale inhibitors react with divalent cations that are either present in the formation or that are injected along with the inhibitor to generate scale inhibitor precipitates. These scale inhibitor precipitates are then slowly dissolved back into the formation water to prevent scale formation. (Rerkpattanapipat *et al.*, 1997) In unsuccessful treatments, most of the inhibitor placed in the formation is not retained and is quickly swept from the formation, resulting in an inefficient use of the inhibitor and a decrease in squeeze lifetime. Consequently, subsequent treatments are required resulting in lost production time and significant cost. Therefore, a successful squeeze treatment is one in which the scale inhibitor is able to slow or prevent scale from forming over long periods of time (Carlberg, 1987).

## 4.3 Background

The precipitation of phosphonate scale inhibitors with calcium has been previously studied in our research group and elsewhere (Kan *et al.*, 1994; Browning and Fogler, 1995; Browning and Fogler, 1996; Rerkpattanapipat *et al.*, 1997; Wattana, 1997; Frostman, 1998; Suwannamek, 1998; Liwsrisakul, 1999). It has been observed that a change in the precipitating conditions can alter the number of calcium cations attached to the phosphonate resulting in the formation of precipitates with markedly different properties. A fundamental understanding of this phenomenon is important in designing squeeze treatments. For example, precipitating conditions that result in formation precipitates with desirable properties

that ensure long squeeze lifetimes (i.e. slow dissolution rates) will result in more effective precipitation squeeze treatments (Browning and Fogler, 1995; Browning and Fogler, 1996; Rerkpattanapipat *et al.* 1997; Wattana, 1997; Suwannamek, 1998; Liwsrisakul, 1999). However, the effect of other cations especially in the formation water on Ca-ATMP precipitates has not been investigated. Mg ions contained in dolomitic formations may influence the formation of Ca-ATMP precipitates resulting in an unsuccessful squeeze treatment. This research was undertaken to identify the range of Mg ion concentrations that affect the precipitation of Ca-ATMP scale inhibitors.

#### **4.4 Materials and Methods**

##### **4.4.1 Materials**

The ATMP scale inhibitor used in this study was supplied by Solutia Co. as an aqueous solution (50% w/w). Each ATMP molecule contains three active phosphate groups. Analytical grade  $\text{CaCl}_2 \cdot 2\text{H}_2\text{O}$ ,  $\text{MgCl}_2 \cdot 6\text{H}_2\text{O}$  and NaCl were obtained from Fisher Scientific Inc. NaCl was used in some experiments to investigate the effect of ionic strength. All stock solutions were made by diluting ATMP or dissolving  $\text{CaCl}_2 \cdot 2\text{H}_2\text{O}$ ,  $\text{MgCl}_2 \cdot 6\text{H}_2\text{O}$  and NaCl in deionized water. Analytical grade KOH and HCl were used for adjusting the solution pH.

##### **4.4.2 Precipitation Experiment**

All precipitation experiments were carried out at room temperature (25°C). The experiment apparatus used for this series of experiments is illustrated in Figure 4.1. The experiment procedures are described briefly as follows. A desired amount of ATMP solution was placed in a spherical flask and stirred continuously by a magnetic stirrer while nitrogen gas was bubbled into solution to avoid a reduction in the solution pH by absorption of carbon dioxide from air. A pH electrode was placed into the solution to monitor the pH throughout the course of an experiment. Deionized water was added to the solution to obtain the desired final concentration of ATMP. Next, a calculated volume of 5M  $\text{CaCl}_2$  solution was slowly added followed by adding either concentrated KOH or HCl as needed to keep the solution pH

constant (1.5, 4 or 7). After 3 days of precipitation process, the solution was found to have a white powdered precipitate. The resulting precipitate was filtered using a 0.22 micron filter membrane, washed with deionized water, dried at 70°C and inspected for the presence of Cl<sup>-</sup> ions using Electron Dispersive X-ray Analyzer (EDX, see Figure 4.2). The procedure for washing and drying was repeated until no Cl<sup>-</sup> ion was detected. The complete removal of chloride was necessary because it can interfere with the determination of precipitate composition.

Mg-ATMP precipitates were prepared using the same procedure as for Ca-ATMP, except that MgCl<sub>2</sub> was used instead of CaCl<sub>2</sub> in the precipitating solution. The Ca-Mg-ATMP precipitation procedures were the same as for Ca-ATMP precipitation, except that MgCl<sub>2</sub> and ATMP solutions were mixed together in a spherical flask before the addition of the CaCl<sub>2</sub> solution. A Mg to Ca molar ratio of the solutions was systematically varied from 0 to 2.35 while keeping both calcium and ATMP concentrations constant. In general, the ATMP concentration was maintained at 0.089 M in the precipitating solution. In some experiments, the concentrations of ATMP and divalent cations in supernatant were measured using Hach technique and Atomic Absorption Spectroscopy (Perkin-Elmer, 3100). With the Hach technique, 10 ml of ATMP solution was oxidized in the presence of persulfate under UV light for 10 min to orthophosphate. The resulting orthophosphate was then reacted with a molybdate blue reagent where the concentrations could then be determined colorimetrically using a UV/Vis spectrophotometer. The amount (%mole) of ATMP precipitated was calculated as the difference between the initial amount of ATMP added and the amount of ATMP in supernatant.

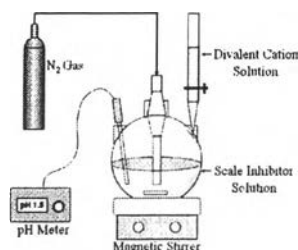


**Figure 4.1** Schematic of apparatus used to synthesize divalent cation-scale inhibitor precipitates.

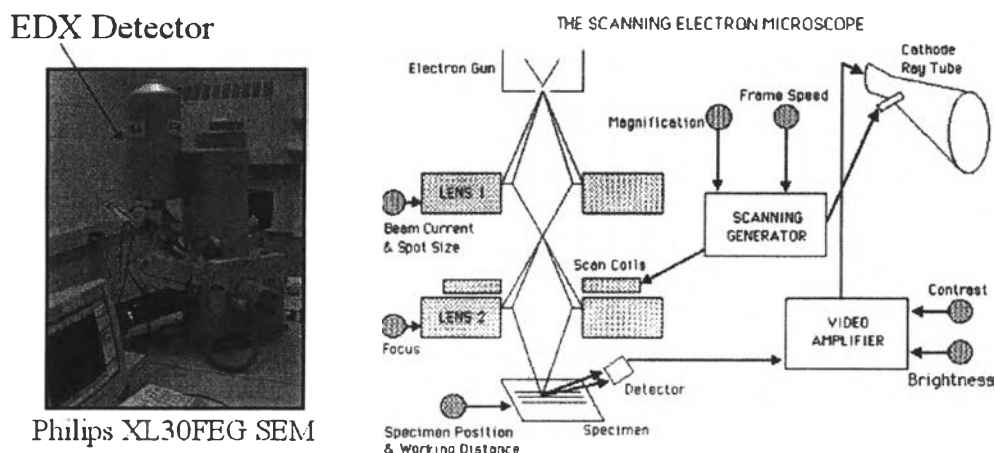


**Figure 4.2** Scanning Electron Microscope.

#### 4.4.3 Characterization of ATMP Precipitates

##### i. Chemical Composition Analysis

The Ca and Mg to ATMP molar ratios in the precipitates were determined by using Atomic Absorption Spectroscopy, and the Hach technique using a UV/Vis spectrophotometer. The results were confirmed using an EDX.

##### ii Morphology and Structure Analysis

The precipitate morphologies were determined by using a SEM (Figure 4.2) and a X-ray Diffractometer (XRD Rigaku 300: 12 kw high intensity rotary anode generator with wide-angle horizontal diffractometer equipped with low-temperature camera).

##### iii Dissolution Experiments

The initial dissolution rate of the precipitate was measured using a rotating disk reactor as shown in Figure 4.3. First, the precipitate powder was molded into a 13 mm diameter thin disk using a hydraulic press at 500 psi and a highly polished stainless steel die. The molded sample surface was inspected by scanning electron microscope and it was found that the surface was smooth and clean. Therefore the effective surface is assumed to be equal to the area of the disk. The molded disk was attached to the center of a rotating disk and rotated at a constant speed of 1000 rpm, which was immersed in 200 ml of deionized water. The concentration of ATMP was measured as a function of time and the initial rate of

ATMP precipitate dissolution was determined. Above 1,000 rpm there was no change in the dissolution rate indicating there were no mass transfer limitations.

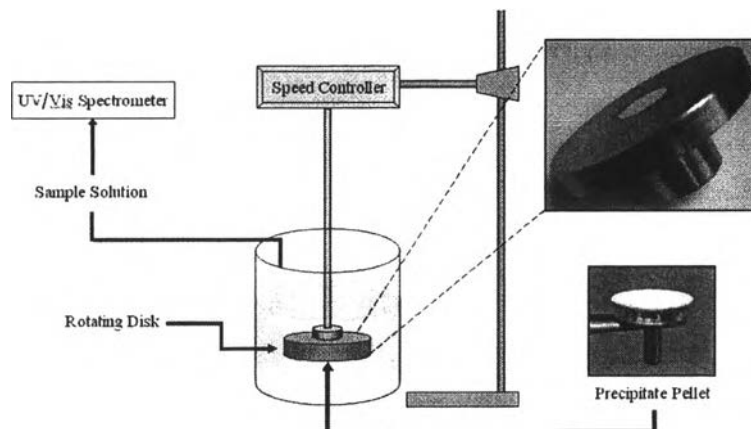


**Figure 4.3** Schematic showing the rotating disk apparatus.

## 4.5 Results and Discussion

The precipitation conditions and the characterization of the precipitates are shown in Table 4.1. Results were obtained for the three types of precipitates, Ca-ATMP, Mg-ATMP and (Ca+Mg)-ATMP. The dissolution rates of the different precipitates were compared to assess the effect of the Mg ion on the rate of dissolution. One of the goals is to determine the conditions affecting Ca-ATMP precipitation, even if the extremes of the conditions might not be typical of those normally found in representative formation waters.

### 4.5.1 ATMP Precipitation with Calcium Ions

Rerkpattanapipat *et al.* (1997) has shown that the precipitating solution pH is one of the important factors affecting the molar ratio of Ca to ATMP in precipitate. As the precipitating solution pH increases, a greater number of hydrogen atoms deprotonate from the ATMP molecule. Consequently, the Ca ion has a greater number of reacting sites available on the ATMP molecule, resulting in an increased Ca to ATMP molar ratio in the precipitate. (Kan *et al.*, 1994) The first set of batch synthesis experiments (experiments 1, 16, and 26) was used to collaborate

Rerkpattanapit's results and was the starting point of this study. For a solution pH of 1.5, one Ca atom precipitated with one ATMP molecule, resulting in a 1:1 Ca-ATMP precipitate. At pH 4 and pH 7, the molar ratios of Ca to ATMP in the precipitates were 2:1 and 3:1 respectively. The mole percentage of ATMP that precipitated out from solution was found to increase with increasing solution pH: 78% for pH 1.5, 87% for pH 4 and 89% for pH 7. Therefore, maintaining a high solution pH during the precipitation squeeze treatment will favor inhibitor retention (precipitation) in the formation matrix, resulting in more efficient use of the injected inhibitor and consequently an increase in squeeze lifetime. The precipitation reactions of ATMP with a divalent cation are shown in Figure 4.4.

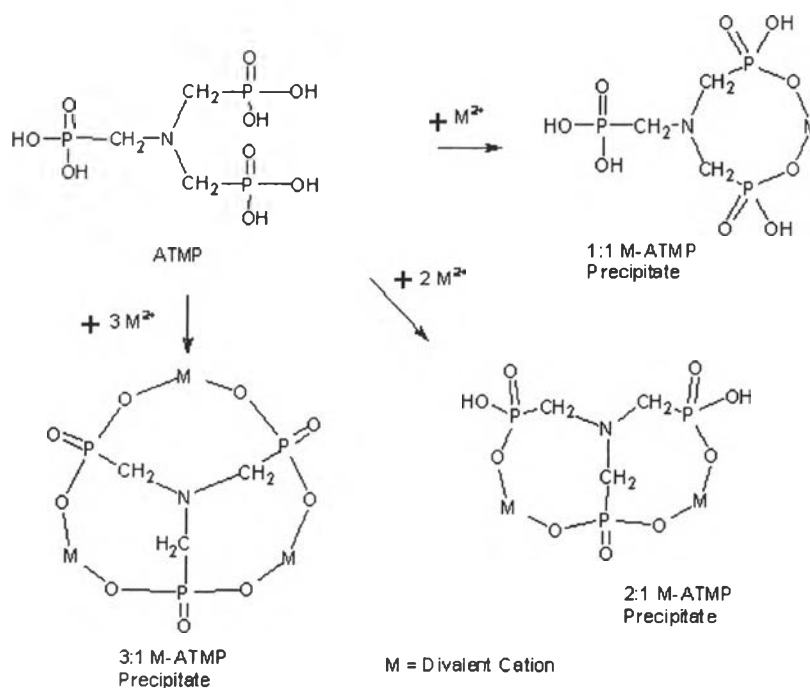


**Figure 4.4** Precipitation reaction mechanisms between divalent cations and ATMP.

**Table 4.1** Summary of batch synthesis and characterization experiments for ATMP precipitates.

Precipitating Conditions:  $[Ca] = 0.894 \text{ M}$ ,  $[ATMP] = 0.089 \text{ M}$ ,  
 $Ca/ATMP = 10:1$  and  $[Ca][ATMP] = 0.08 \text{ M}^2$

Exp.#	Precipitating Solution Conditions					Precipitate Characterizations						Morphologies	Structure
	pH	[Mg] (M)	[Mg].[ATMP] (M <sup>2</sup> )	Mg/Ca molar ratio	Ionic Strength (M)	Ca/ATMP molar ratio	Mg/ATMP molar ratio	Ca Mg/ATMP molar ratio	(Ca+Mg)/ATMP molar ratio	Mg/Ca molar ratio			
1	1.5	0.00	0.00	no Mg	2.68	1.04	-	1.04:0.00/1	1.04	-	Flake	Crystalline	
2	1.5	0.18	0.02	0.20	3.22	1.12	0.09	1.12:0.09/1	1.21	0.08	XXXXX	XXXXX	
3	1.5	0.45	0.04	0.50	4.02	1.09	0.05	1.09:0.05/1	1.14	0.05	XXXXX	XXXXX	
4	1.5	0.89	0.08	1.00	5.36	1.04	0.07	1.04:0.07/1	1.11	0.07	Flake	Crystalline	
5	1.5	1.19	0.11	1.33	6.26	0.84	0.14	0.84:0.14/1	0.98	0.17	XXXXX	XXXXX	
6	1.5	1.43	0.13	1.60	6.98	1.01	0.28	1.01:0.28/1	1.29	0.28	XXXXX	XXXXX	
7	1.5	1.52	0.135	1.70	7.25	1.18	0.05	1.18:0.05/1	1.23	0.04	XXXXX	XXXXX	
8	1.5	1.61	0.143	1.80	7.51	0.97	0.07	0.97:0.07/1	1.04	0.07	XXXXX	XXXXX	
9	1.5	1.70	0.15	1.90	7.78	1.05	0.13	1.05:0.13/1	1.18	0.12	XXXXX	XXXXX	
10	1.5	1.79	0.16	2.00	8.05	1.21	0.90	1.21:0.90/1	2.11	0.74	Spherical	Amorphous	
11	1.5	2.10	0.19	2.35	8.99	1.21	1.07	1.21:1.08/1	2.28	0.88	XXXXX	XXXXX	
12	1.5	0.89	0.08	no Ca	2.68	-	*****	*****	*****	-	*****	*****	
13	1.5	2.83	0.80	no Ca	8.49	-	1.10	0.00:1.10/1	1.10	-	Flake	Crystalline	
14	1.5	2.92	0.85	no Ca	8.75	-	1.19	0.00:1.19/1	1.19	-	Flake	Crystalline	
15	1.5	0.89	0.08	NaCl, no Ca	5.37	-	1.04	0.00:1.04/1	1.04	-	Flake	Crystalline	
16	4.0	0.00	0.00	no Mg	2.68	2.06	-	2.06:0.00/1	2.06	-	Spherical	Amorphous	
17	4.0	0.18	0.02	0.20	3.22	1.78	0.40	1.78:0.40/1	2.18	0.22	XXXXX	XXXXX	
18	4.0	0.45	0.04	0.50	4.02	1.54	0.70	1.54:0.70/1	2.24	0.45	XXXXX	XXXXX	
19	4.0	0.89	0.08	1.00	5.36	1.33	1.04	1.33:1.04/1	2.37	0.78	Spherical	Amorphous	
20	4.0	1.79	0.16	2.00	8.05	*****	*****	*****	*****	*****	*****	*****	
21	4.0	0.89	0.08	no Ca	2.68	-	*****	*****	*****	-	*****	*****	
22	4.0	1.00	0.10	no Ca	3.00	-	*****	*****	*****	-	*****	*****	
23	4.0	2.24	0.50	no Ca	6.72	Formation of Mg(OH) <sub>2</sub>				XXXXX	XXXXX		
24	4.0	2.83	0.80	no Ca	8.49	Formation of Mg(OH) <sub>2</sub>				XXXXX	XXXXX		
25	4.0	0.89	0.08	NaCl, no Ca	5.37	-	2.29	0.00:2.29/1	2.29	-	Spherical	Amorphous	
26	7.0	0.00	0.00	no Mg	2.68	3.04	-	3.11:0.00/1	3.04	-	Spherical	Amorphous	
27	7.0	0.18	0.02	0.20	3.22	2.44	0.57	2.44:0.57/1	3.01	0.23	XXXXX	XXXXX	
28	7.0	0.45	0.04	0.50	4.02	2.19	0.93	2.19:0.93/1	3.12	0.42	XXXXX	XXXXX	
29	7.0	0.89	0.08	1.00	5.36	1.89	1.41	1.89:1.41/1	3.30	0.75	Spherical	Amorphous	
30	7.0	1.79	0.15	2.00	8.05	1.28	1.80	1.28:1.80/1	3.08	1.41	XXXXX	XXXXX	
31	7.0	0.71	0.05	no Ca	2.12	-	*****	*****	*****	-	*****	*****	
32	7.0	0.89	0.08	no Ca	2.68	-	*****	*****	*****	-	*****	*****	
33	7.0	2.24	0.50	no Ca	6.72	Formation of Mg(OH) <sub>2</sub>				XXXXX	XXXXX		
34	7.0	2.83	0.80	no Ca	8.49	Formation of Mg(OH) <sub>2</sub>				XXXXX	XXXXX		
35	7.0	0.89	0.08	NaCl, no Ca	5.37	-	3.04	0.00:3.04/1	3.04	-	Spherical	Amorphous	

\*\*\*\*\* No precipitates formed at this condition XXXXX Analysis not carried out

#### 4.5.2 ATMP Precipitation with Magnesium Ions

At a pH of 1.5, no Mg-ATMP precipitate was formed, even after one month, at a molar product  $[Mg].[ATMP]$  of  $0.08 \text{ M}^2$  (experiment 12), while a molar product  $[Ca].[ATMP]$  of  $0.08 \text{ M}^2$  was sufficient to form a 1:1 Ca-ATMP precipitate (experiment 1) immediately after mixing. To obtain a 1:1 Mg-ATMP precipitate, the molar product  $[Mg].[ATMP]$  had to be increased 10 times to  $0.8 \text{ M}^2$  where the ionic strength was 8.49 M. The solubility product  $[Mg].[ATMP]$  of 1:1 Mg-ATMP was



found to be  $0.049 \text{ M}^2$ , which is approximately three times that of 1:1 Ca-ATMP ( $[\text{Ca}].[ATMP]=0.017 \text{ M}^2$ ).

For values of the molar product  $[\text{Mg}].[ATMP]$  less than  $0.10 \text{ M}^2$  and an ionic strength of 2.7 M or lower, no Mg-ATMP precipitates were observed at either a solution pH 4 or pH 7 (c.f. experiments 21, 22, 31 and 32). Increasing the molar product at these pH values resulted in the formation of magnesium hydroxide  $\text{Mg}(\text{OH})_2$  which interferes with the analysis of the precipitates. However, Mg-ATMP precipitates were formed at a molar product  $[\text{Mg}].[ATMP]$  of  $0.08 \text{ M}^2$  in the presence of NaCl in solutions at an ionic strength of 5.36 M (c.f. experiments 15, 25 and 35). The molar ratios of Mg to ATMP in the Mg-ATMP precipitates formed were 1:1, 2:1 and 3:1 at solution pH values of 1.5, 4.0 and 7.0, respectively. This important result shows that a high ionic strength is necessary to obtain Mg-ATMP precipitates. The formation of Mg-ATMP precipitate at high ionic strengths may be due to a decrease in solubility of Mg-ATMP precipitate (salting-out) at high ionic strengths.

To determine the effect of ionic strength on the apparent solubility of Mg-ATMP precipitates, the precipitation procedure discussed in a previous section, 4.3.2, was used, except that the ionic strength was varied by adding NaCl to the solution. The ATMP and divalent cation concentrations in the supernatant were measured at least one week after the precipitates were formed to ensure equilibrium was reached. The apparent solubilities of ATMP precipitates were calculated using the equation:

$$S = \sqrt[m+1]{[M]^m \cdot [ATMP]}, \quad (4.1)$$

where  $[M]$  and  $[ATMP]$  are the concentrations of  $\text{MgCl}_2$  and ATMP in the supernatant (M), respectively, and  $m$  is the molar ratio of cations to ATMP in the precipitates.

An analysis of the precipitates showed that up to a NaCl concentration of 3 M, the presence of NaCl in solution does not affect the molar ratio of Mg to ATMP in the precipitates. In addition, no Na ions were found in the precipitates. It was found that the apparent solubility ( $S$ ) of the Mg-ATMP decrease with the addition of

NaCl. The logarithm of the apparent solubility varies linearly with the salinity, consistent with the theory proposed by Setchenow. The Setchenow coefficient ( $k_s$ , in  $M^{-1}$ ) is calculated using the following equation (Harned and Owen, 1950):

$$\log S = -k_s C + \log S^o, \quad (4.2)$$

where  $S$  and  $S^o$  are the apparent solubilities (M) in the presence of salt and in pure water, respectively, and  $C$  is the salinity. Because of the low solubility of ATMP, its contribution to the total salinity of the solution is negligible. The salinity is just the sum of the NaCl and  $MgCl_2$  concentration in the solution. The value of  $k_s$  is obtained from the slope of a plot of  $\log S$  as a function of  $C$  while the values of  $S^o$  is obtained from the intercept.

A similar salting out effect was also observed for the precipitation of Ca-ATMP. The experimental procedure and solubility calculation were similar to that for the Mg-ATMP precipitates.

The values of  $k_s$  and  $S^o$  of ATMP precipitates are given in Table 4.2. A positive value of  $k_s$  indicates a decrease in solubility (salting out) whereas a negative value of  $k_s$  indicates an increase in solubility of the solute (salting in) upon addition of salt. It was shown that, cation-ATMP salt out in a reservoir having regions of high salinity because the Setchenow coefficient values of ATMP precipitates are all positive. An increase in salinity decreases the solubility of 3:1 Ca-ATMP more than that of the 2:1 and 1:1 Ca-ATMP precipitates. Similarly an increase in salinity decreases the solubility of 1:1 Mg-ATMP more than that of the 2:1 and 3:1 Mg-ATMP. A number of models used to predict the value of  $k_s$  were recently reviewed by Millero 2000. (Millero 2000) Unfortunately, none of the models can be applied to the cation-ATMP system since models because they require a number of parameters such as polarizability and mixing potential that are not readily available for our system. Therefore an estimated value of  $k_s$  is not possible. It was found that the values of  $S^o$  for Mg-ATMP precipitates are greater than those for Ca-ATMP precipitates for the same molar ratio of cations to ATMP as shown in Table 4.2.

**Table 4.2** Summary of the values of  $k_s$  and  $S^o$  of ATMP precipitates.

Type of precipitate	$k_s$ ( $M^{-1}$ )	$S^o$ (M)	Type of precipitate	$k_s$ ( $M^{-1}$ )	$S^o$ (M)
1:1 Ca-ATMP	0.020	0.14	2:1 Mg-ATMP	0.045	0.47
1:1 Mg-ATMP	0.079	0.23	3:1 Ca-ATMP	0.066	0.37
2:1 Ca-ATMP	0.015	0.23	3:1 Mg-ATMP	0.047	0.55

#### 4.5.3 ATMP Precipitation with Ca and Mg

The effect of Mg ion on Ca-ATMP precipitation was studied by keeping the concentrations of ATMP and  $CaCl_2$  constant at the previous values of 0.089 M and 0.89 M, respectively and by maintaining a 1:1 molar ratio of Ca to Mg in solution in all the experiments. The amount of ATMP precipitated in the system with and without Mg is compared in Figure 4.5. The results show that the amount of ATMP precipitated decreased with the addition of Mg at all solution pH values suggesting that the presence of Mg decreases the effectiveness of Ca-ATMP precipitation and enhance the squeeze treatment. For example, at solution pH of 1.5, the percentage of ATMP precipitated out from solution decreased from 78% in the absence of Mg to 42% in the presence of Mg ion. This smaller amount of ATMP precipitated may be a result of an increase in Mg-ATMP complex in the liquid phase. Consequently, the effect of Mg ions can be profound in reservoirs that have significant dolomite content. Under these conditions, most of the scale inhibitor may not be retained in the formation and consequently the scale inhibitor will quickly swept out into produced water during start up, resulting in insufficient use of the scale inhibitor. The effect of other divalent cations such as Ba and Sr ions to inhibitor precipitation is one part of our ongoing works.

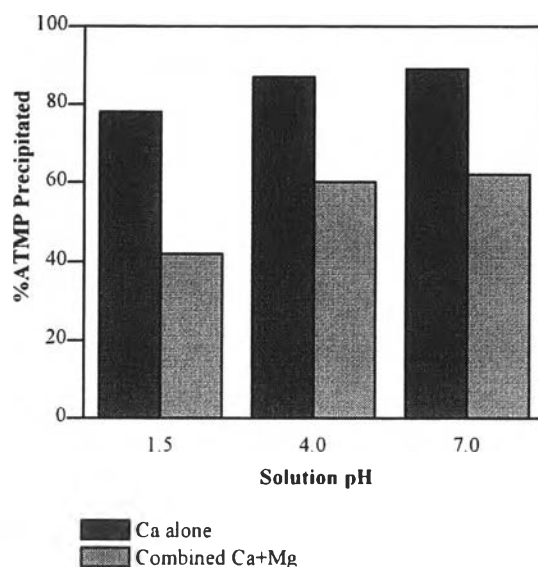
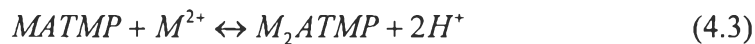


**Figure 4.5** Effect of Mg ions on the amount of ATMP precipitated.

The effect of Mg ion on Ca-ATMP precipitation was also examined by varying the Mg to Ca molar ratios in solution along with the solution pH. Close examination of Table 4.1 reveals several interesting phenomena, which are discussed below.

i Precipitation at pH 1.5

Experiments 1 through 9 in Table 4.1 were all carried out keeping the solution pH constant at 1.5. The initial molar ratio of Mg to Ca in the solutions was less than 2. The elemental analysis showed only a small amount of Mg in these precipitates while the Ca to ATMP molar ratios in the precipitates were approximately constant at 1:1, indicating that the Mg ion had little or no effect on the composition of Ca-ATMP precipitates. Small amounts of Mg (generally <10% mole Mg) observed in some of the precipitates may have resulted from Mg being captured during the Ca-ATMP precipitation. The precipitation of only Ca-ATMP is due to the lower solubility of Ca-ATMP when compared to Mg-ATMP. However, for higher molar ratios of Mg to Ca in solution ( $>2$ ), a 2:1 (Ca+Mg)-ATMP precipitate was formed. The formation of 2:1 (Ca+Mg)-ATMP precipitate from 1:1 Ca-ATMP precipitate could result from the following reaction, (M = Ca or Mg):



The 2:1 precipitate forms by substituting two protons of M-ATMP with a divalent cation. From Equation 4.3, one observes a decrease in hydrogen activity or an increase in the divalent cation activity favors the formation of the 2:1 precipitate. The addition of Mg ions to the solution results in the transformation of 1:1 to 2:1 precipitate by shifting the reaction to the right. At a constant pH, the transformation phenomenon of a 1:1 to a 2:1 precipitate is controlled by the activity of divalent cations. Furthermore, the inhibitor precipitation kinetics under a variety of precipitating conditions such as in Ba and Sr solutions will be describe in Chapter V.

#### ii Precipitates at pH 4

Figure 4.6 shows the molar ratio of the divalent cations to ATMP in the precipitates obtained from experiments 16 to 19. Under the studied conditions, that the Ca to ATMP molar ratio in the precipitates decreases with increasing Mg concentration in solution. These results indicate that Mg and Ca compete for the same reacting sites on ATMP molecules. The number of ATMP molecules tied up with Mg ions increased with increasing Mg concentration resulting in a lower Ca to ATMP molar ratio in the precipitates. At a constant pH of 4, the molar ratio of (Ca+Mg) to ATMP in the precipitates remained constant at approximately 2:1. Moreover, the percentage of ATMP precipitated decreased from 87% in the absence of Mg (experiment 16) to 60% in the presence of Mg (experiment 19). As a result, the presence of Mg will cause shorter squeeze lifetimes. Up to a Mg to Ca molar ratio of 2 in solution, no ATMP precipitates were formed (experiment 20). Consequently, no ATMP would be retained in the formation as precipitates under these conditions.

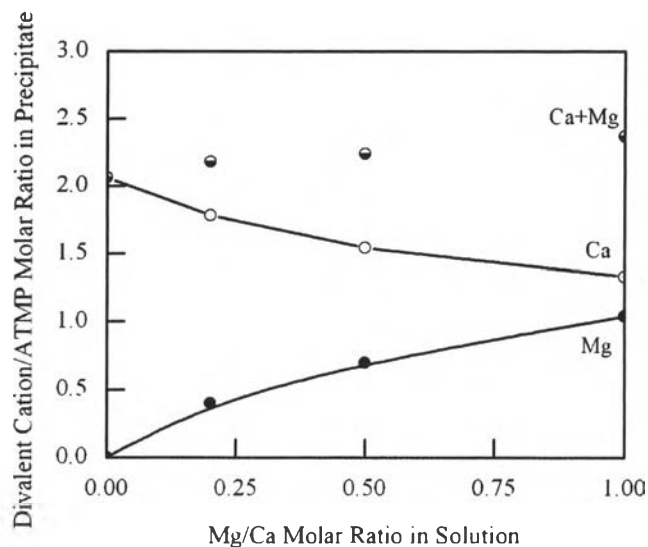


**Figure 4.6** Effect of increasing Mg concentration in the solution on the composition of precipitate at pH 4.0 and  $[Ca][ATMP] = 0.08 \text{ M}^2$ .

### iii Precipitates at pH 7

A phenomenon similar to the results at solution pH 4 was observed in the precipitates formed at solution pH 7 when the Mg to Ca molar ratio was varied from 0 to 2.0 (c.f. experiment 26-30). At pH 7, the most stable structure of the precipitates contained three divalent cations bonded with one ATMP molecule, that is, a 3:1 molar ratio of total divalent cations to ATMP in the precipitates. The results show that the percentage of ATMP precipitated from solution decreased from 89% (experiment 26) in the absence of Mg to 62% in the presence of Mg (experiment 29) while all other conditions remained the same.

#### 4.5.4 Type of Precipitates

Two possible bonding structures for the Ca-Mg-ATMP system are co-precipitates and complex precipitates. Co-precipitates are formed by a mixture of different divalent cation-scale inhibitor precipitates (e.g. Ca-ATMP and Mg-ATMP precipitates) with no attachment of Ca and Mg on the same ATMP molecule. With complex precipitates, both Mg and Ca divalent cations attach to the active phosphate

groups on the same molecule of ATMP. At a  $[Mg].[ATMP]$  molar product of  $0.08 \text{ M}^2$  and a solution pH of 4, Mg-ATMP did not precipitate in a Ca free solution (c.f. experiment 21). However at the same pH (pH 4), it was found that Mg ions precipitated with ATMP when both Ca and Mg were each at a molar product of  $0.08 \text{ M}^2$  (i.e.,  $[Ca].[ATMP] = 0.08 \text{ M}^2$  and  $[Mg].[ATMP] = 0.08 \text{ M}^2$ ). Mg ions may precipitate by bonding with a stable Ca-ATMP precipitate to form a complex precipitate of (Ca+Mg)-ATMP. Similar results were also obtained at pH 7. The precipitates may not be co-precipitates of  $\text{Ca}_2\text{ATMP}$  and  $\text{Mg}_2\text{ATMP}$  but instead either complex precipitates of Ca-Mg-ATMP or a mixture of co-precipitates and complex precipitates.

#### 4.5.5 Morphology and Structure

It is apparent that differences in precipitating conditions resulted in different compositions of precipitates. Moreover, a change in precipitating conditions results in a difference in precipitate shape, size and crystallinity. The different ATMP precipitate morphologies are shown in Figure 4.7. The precipitates of both 1:1 Ca-ATMP and 1:1 (Ca+Mg)-ATMP form flake or plate-like particles. While the 1:1 Mg-ATMP precipitate forms an irregular shape and flake particles, the 2:1 and 3:1 of Ca-ATMP, Mg-ATMP and (Ca+Mg)-ATMP precipitates form powdery spherical particles. A comparison of 1:1 (Ca+Mg)-ATMP precipitate morphology with 1:1 Ca-ATMP precipitate morphology reveals a similar plate like shape, but smaller in particle size for the 1:1 (Ca+Mg)-ATMP precipitate. However, it is possible that size and morphologies of scale inhibitor precipitates observed in batch experiments might be different than those formed in a porous media or natural mineral surfaces.

The X-ray diffraction (XRD) pattern for the precipitates in Figure 4.7 is shown in Figure 4.8. The XRD pattern of the 1:1 Ca-ATMP precipitate shows sharp peaks at  $2\theta$  values of  $9.5^\circ$ ,  $10.5^\circ$  and  $18.5^\circ$ , while those of a 1:1 Mg-ATMP precipitate show sharp peaks at  $2\theta$  values of  $12.5^\circ$ ,  $15.5^\circ$  and  $18.6^\circ$ , indicating a crystalline structure. The position of XRD peaks for the 1:1 Ca-ATMP precipitates are not the same as those for Mg-ATMP, indicating the structures of Ca-ATMP and Mg-ATMP precipitates are different. The XRD analysis on 2:1 and 3:1 of Ca-ATMP,

Mg-ATMP and (Ca+Mg)-ATMP precipitates showed essentially no peaks, indicating an amorphous structure. The XRD pattern of 1:1 (Ca+Mg)-ATMP at Mg to Ca molar ratio of 1.0 in solution (experiment 4) shows sharp peaks at  $2\theta$  values of  $10.5^\circ$  and  $18.5^\circ$  which are similar to those obtained for 1:1 Ca-ATMP precipitate.

#### 4.5.6 Dissolution Rates

Batch dissolution experiments were carried out to further characterize the cation-ATMP precipitates using a rotating disk reactor. A slow dissolution rate of ATMP precipitate will result in longer squeeze lifetimes and will enhance the success of a squeeze treatment. The dissolution rate of the precipitates was calculated from the number of ATMP moles dissolved per unit pellet surface area per time. Table 4.3 shows a comparison of the dissolution rates for different molar ratios of the divalent cation to ATMP in the precipitates. While the dissolution of the 1:1 Mg-ATMP precipitate was virtually instantaneous, the dissolution of the 3:1 (Ca+Mg)-ATMP precipitate was slowest. The dissolution rate of ATMP precipitates decreases significantly with an increasing molar ratio of divalent cation to ATMP in the precipitates. These results are in accord with previous studies with Ca-ATMP precipitates that were based on the rate of ATMP released in micro model experiments.(Kan *et al.*, 1994) It is important to note that the dissolution rate of the inhibitor might be different in brine for actual field applications. The presence of other salts in a reservoir fluid might also affect the inhibitor dissolution rate.



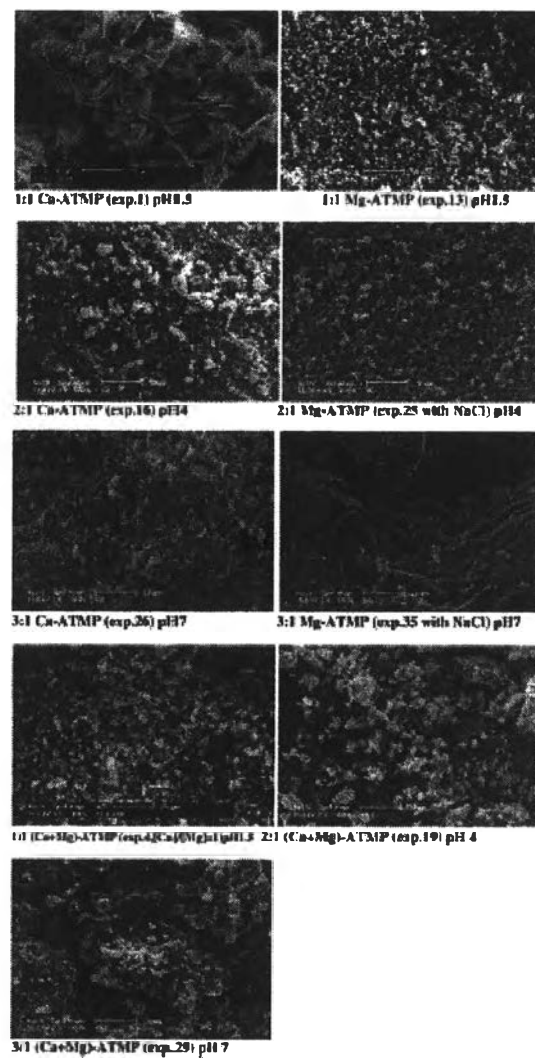


**Figure 4.7** Morphologies of ATMP precipitates from different precipitating conditions.

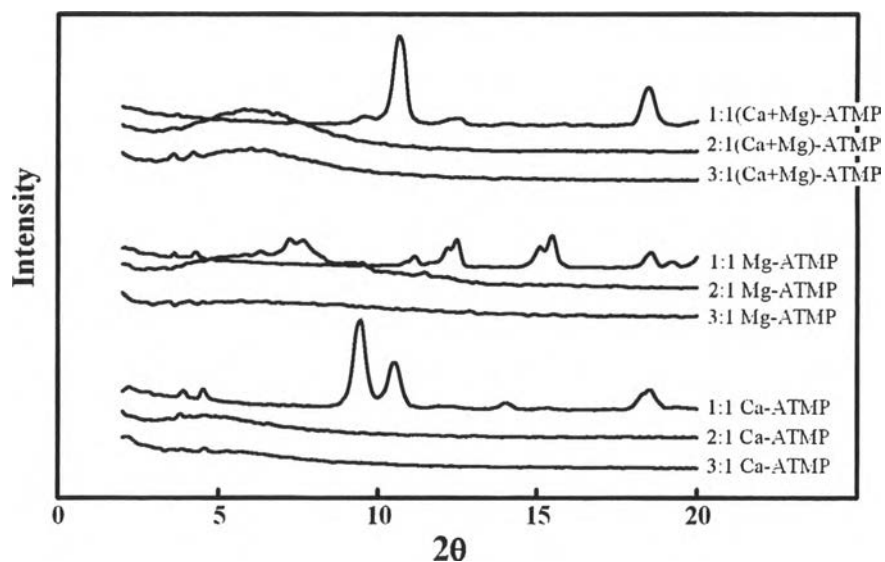


**Figure 4.8** XRD pattern of ATMP precipitates from different precipitating conditions.

**Table 4.3** Summary of rotating disk dissolution rates of three types of precipitates.

Type of Precipitate	Dissolution Rates (mol.ATMP/cm <sup>2</sup> .min)
1:1 Ca-ATMP	2.38
1:1 Mg-ATMP	Virtually instantaneous
2:1 Ca-ATMP	0.14
2:1 Mg-ATMP	0.11
2:1 (Ca+Mg)-ATMP	0.10
3:1 Ca-ATMP	0.04
3:1 Mg-ATMP	0.04
3:1 (Ca+Mg)-ATMP	0.03

## 4.6 Conclusions

Precipitation of Cations-ATMP scale inhibitors were studied in batch experiments. The morphologies and structure of precipitates of Ca-ATMP, Mg-ATMP, and (Ca+Mg)-ATMP were examined by SEM and XRD. After characterization, the dissolution rates of the precipitates were studied using a rotating disk reactor.

i. The molar ratio of divalent cations to ATMP molecules in the precipitate increased with increasing pH of the precipitating solution.

ii. The molar product required for Mg-ATMP to form a precipitate was greater than that of Ca-ATMP and a high ionic strength was required to form Mg-ATMP precipitates.

iii. The amount of ATMP precipitated increased with increasing solution pH and decreased when Mg ions were added to the solutions.

iv. The molar ratio Mg to ATMP in the precipitates increased with an increase in the molar ratio of Mg to Ca in solution at pH values of 4 and 7.

v. The dissolution rate of the divalent cation-ATMP precipitates in deionized water decreased significantly with an increase in molar ratio of divalent cations to ATMP in the precipitates.

vi. The amount of ATMP precipitated and the dissolution rate suggest that a squeeze treatment at pH 7 in a Mg-free solution will provide longest squeeze lifetime compared to lifetime at pH 1.5 and pH 4. The reason is that the amount of precipitate at pH 7 was greater and the dissolution rate was slower when compared to precipitates formed at pH 1.5 and pH 4. However, the actual squeeze treatment is very complicated process. Squeezing pH 7 brines containing ATMP and high Ca ions would generate a desirable precipitated product, but precipitation likely would occur faster than desired. Therefore, further study on kinetic precipitation of scale inhibitor would be beneficial for effective inhibitor design in order to control the precipitation at desire period and location.

#### 4.7 References

- Browning, F. H. and Fogler, H. S. (1995) Effect of synthesis parameters on the properties of calcium phosphonate precipitates. Langmuir, 11(10), 4143-4152.
- Browning, F. H. and Fogler, H. S. (1995) Precipitation and dissolution of calcium phosphonates for the enhancement of squeeze lifetimes. SPE Production & Facilities, 10(3), 144-150.
- Browning, F. H. and Fogler, H. S. (1996). Effect of precipitating conditions on the formation of calcium-HEDP precipitates. Langmuir, 12(21), 5231-5238.
- Carlberg, B. L. (1987). Scale Inhibitor Precipitation Squeeze for Non-Carbonate Reservoirs. SPE Production Technology Symposium, Lubbock, Texas, USA.
- Frostman, L. M., Kan, A. T., Tomson, M. B. (1998) Mechanistic aspects of calcium phosphonates precipitation. Calcium Phosphates in Biological and Industrial Systems, Z. Amjad. Boston, Kluwer Academic Publishers.
- Harned, H. S. and Owen, B. B. (1950) The physical chemistry of electrolytic solutions. Reinhold Pub., New York.
- Kan, A. T., Oddo, J. E. and Tomson, M. B. (1994) Formation of 2 calcium diethylenetriaminepentakis(methylene phosphonic acid) precipitates and their physical-chemical properties. Langmuir, 10(5), 1450-1455.
- Liwsrisakul, J. (1999). Precipitation, Transformation and re-dissolution of calcium scale inhibitor in porous media. Master Thesis: The Petroleum and Petrochemical College, Chulalongkorn University, Bangkok, Thailand.
- Millero, F. (2000) The activity coefficients of non-electrolytes in seawater Marine Chemistry, 70(1-3), 5-22.
- Oddo, J. E. and Tomson, M. B. (1994) Algorithms can predict - inhibitors can control norm scale. Oil & Gas Journal, 92(1), 33-37.
- Rerkpattanapipat, P., Chavadej, S., Browning, H., and Fogler H. S. (1997) Precipitation and dissolution of calcium-ATMP precipitates for the inhibition of scale formation in porous media. Langmuir, 13, 1791-1798.

- Suwannamek, I. (1998). Dissolution of scale inhibitor (DTPMPA) in porous media. Master Thesis: The Petroleum and Petrochemical College, Chulalongkorn University, Bangkok, Thailand.
- Wattana, P. (1997). Dissolution kinetics of scale inhibitors in the presence of high concentration of calcium. Master Thesis: The Petroleum and Petrochemical College, Chulalongkorn University, Bangkok, Thailand.